Synthesis of colorless imide hybrid nanocomposites using amine functionalized oligosiloxane nano-building clusters

Tae-Ho Lee, Jeong Hwan Kim and Byeong-Soo Bae*

Received 21st December 2005, Accepted 9th February 2006
First published as an Advance Article on the web 20th February 2006
DOI: 10.1039/b518034a

Colorless imide hybrid nanocomposites are fabricated using new amine functionalized oligosiloxane nano-building clusters (AONC) and the cross-linking agent 5-(2,5-dioxotetrahydrofuryl)-3-methyl-cyclohexene-1,2-dicarboxylic anhydride (DODCA) or 1,2,3,4-cyclobutanetetracarboxylic dianhydride (CBDA) in order to obtain thermally stable and optically transparent materials. AONC are cross-linked by short diimide bonds which were formed by reaction of AONC with alicyclic dianhydrides and the fabricated nanocomposites have 3-dimensional network structures. The prepared nanocomposites show good thermal stability with 5% weight loss temperature around 430 °C and excellent optical properties such as colorlessness (optical transmission of above 90% in the visible region and ultraviolet cut-off around 310 nm), large modulation of refractive index and low birefringence (about 0.002). Colorless imide hybrid nanocomposites prepared from AONC and alicyclic dianhydride (DODCA and CBDA) are potential materials for optical and opto-electronic applications.

Introduction

The fabrication of inorganic–organic hybrid nanocomposites (IOHN) using nano-building clusters has attracted a lot of attention over the last decade due to their potential in applications as varied as smart coatings, insulation layers in electronics and host materials in rare-earth complex and organic dye doping.[1–5] The IOHN prepared from siloxane-based nano-building clusters such as polyhedral oligomeric silsesquioxanes (POSS) or metal-oxo-clusters containing siloxanes allow more precise control of their nanostructures and better reproducibility of their properties compared to conventional IOHN in which inorganic and organic are mixed at the nanosize level.[6,7] In particular, POSS derived from the hydrolytic condensation of trifunctional organo-silicon monomers have offered these advantageous features in the construction of IOHN. However, their synthesis and functionalization by introducing functional organic groups, such as methacrylates, epoxides and amines, required complicate chemical modification.[1,8] Thus, the simple synthesis of siloxane-based nano-building clusters, in which their further growth or agglomeration is prevented, is essential for the easy and reproducible fabrication of IOHN.

POSS usually exist as a solid powder so they have to be dissolved in proper organic solvents for additional uses. The choices of solvents and catalysts have to be carefully considered in both the fabrication of IOHN utilizing POSS and chemical functionalization of POSS. Thus, the synthesis of new solventless-liquid nano-building clusters, which can replace POSS, is required for versatile synthetic routes.

Laboratory of Optical Materials and Coating (LOMC), Department of Materials Science and Engineering, Korea Advanced Institute of Science and Technology (KAIST), Daejeon 305–701, Republic of Korea. E-mail: bsbae@kaist.ac.kr; Fax: +82 42 869 3310; Tel: +82 42 869 4119

Generally, the introduction of aminopropyl or aminophenyl, which are very important and promising functions in binding sites for DNA, microcrystals, diamond surfaces and photo-functional organic molecules, into POSS or nano-building clusters were conducted by many chemical synthetic steps such as hydrolysis, condensation, hydrosilylation, bromination, nitration, neutralization and precipitation and so on.[1,8–13] Since the terminated $–NH_2$ ligands are positively chargeable in neutral to acidic media, neutralization of NH_3^+ to NH_2 is necessary to obtain amino functionality. However, they are very difficult to neutralize without destroying the siloxane backbone in nano-building clusters by soaking in strong acid solution. Neutralization using ion exchange was proposed as a alternative method but this method also needed various chemical treatments.[8,13] Thus, simple amine-functionalization without neutralization has to be developed in the synthesis of new siloxane-based nano-building clusters.

In this paper, amine functionalized oligosiloxane nano-building clusters (AONC) were synthesized using a simple condensation reaction (Scheme 1). They have the advantages of POSS in view of novel property tailoring. The most fascinating point of AONC is that they are very easily synthesized and required no additional chemical treatments to maintain their amino functionality. Their sizes and physical properties can be easily controlled by compositional changes. They have great optical properties such as high optical transparency over 90% in the visible light range and easy modulation of refractive index. Also, their excellent ability to form thin or thick films, because of the viscous liquid state, promises easy integration into devices.

Polyimides are a class of polymer used extensively in microelectronics because of their outstanding properties, such as thermoxidative stability, high mechanical strength, and excellent electrical properties.[14] They are used as interlayer dielectrics in integrated circuits. Recently, researchers have

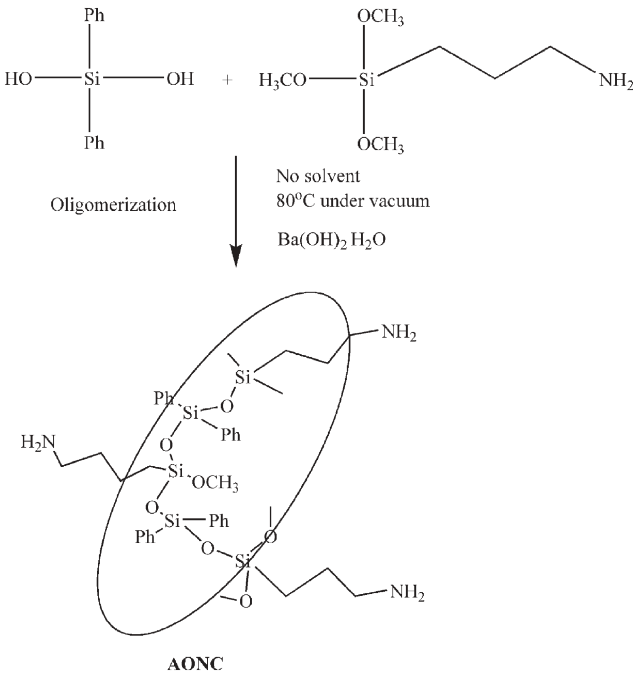

Scheme 1 The synthetic route and reaction scheme of AONC.

extensively studied the opto-electronic and optical applications of polyimides, for example, waveguide materials,[15] low dielectric constant materials[16] and photochromic materials.[17] However, conventional fully aromatic polyimides can be applied to only limited areas due to their high birefringence, low transparency and poor tunability of the refractive index.

In a variety of approaches, researchers have tried to enhance the optical properties of polyimides by changing their structure. The synthesis of semiaromatic polyimides is one of the common approaches.[18] Although they showed the higher transparency, lower birefringence and reduced dielectric constant, because they hardly form inter-or intramolecular charge-transfer complexes,[19] poor mechanical properties restricted their uses. Another approach is to fabricate polyimide/imide hybrid nanocomposites from nano-building clusters such as POSS and AONC.[20] By covalently combining POSS with polyimides or diimide we can effectively enhance the optical characteristics of polyimides without degrading mechanical properties. Furthermore, because the incorporation of POSS reduced the molecular density as well as aggregation between the polyimide chains, we can obtain lower birefringences and dielectric constants. Moreover, the incorporated siloxane-based nano-building clusters enhance optical transparency and thermal stability of nanocomposites. However, in this approach, the refractive index, which is the most important parameter in optical design, is difficult to control within a wide range. We can modulate the refractive index of polyimide-POSS hybrid nanocomposites by varying either the concentration of incorporated POSS or the molecular structure of the dianhydrides. As a result, we varied the refractive index by changing the POSS concentration within a narrow range.

As mentioned, the refractive indices of newly synthesized AONC can vary widely depending on compositional change. Because AONC were covalently bonded to the polyimides, we could incorporate the high concentration of the AONC due to the good compatibility between the AONC and the polyimides. Thus, imide hybrid nanocomposites with AONC can have a large tunability of the refractive index.

Using AONC and alicyclic dianhydrides (Scheme 2), we fabricated new imide hybrid nanocomposites. These nanocomposites combine the advantages of two general approaches, and they have excellent optical properties, such as high, colorless transparency; low birefringence; and large modulation of the refractive index.

To synthesize the imide hybrid nanocomposites from AONC and alicyclic dianhydrides, we used the following three

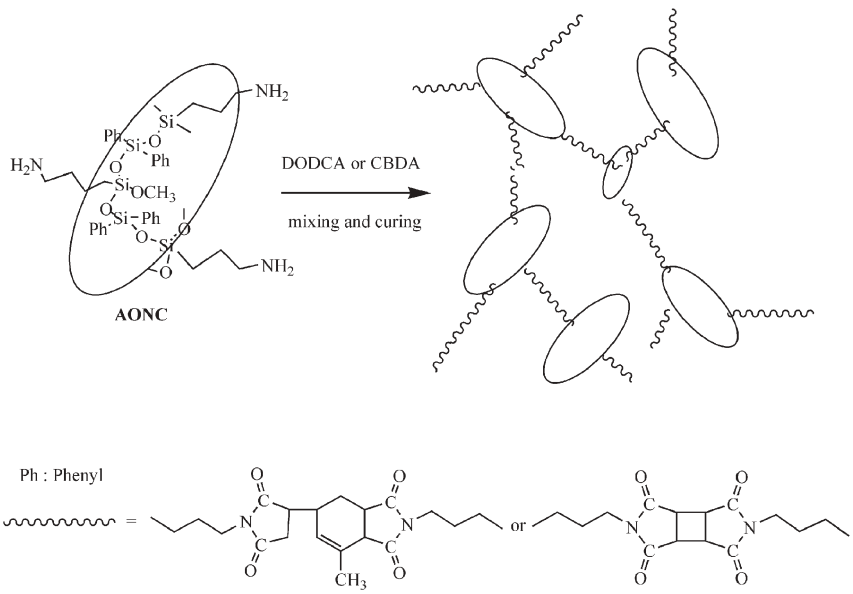

Scheme 2 The imide nanocomposite prepared from AONC and alicyclic dianhydrides as cross-linkers. The three-dimensional network structure in which each AONC is cross-linked by short diimide chains is shown.

steps. First, we synthesized the AONC as described elsewhere. Second, we covalently bonded the AONC with dianhydrides, producing three-dimensional networks with amide linkages. Finally, to form the imide hybrid nanocomposites, we used an optimal imidization process, which uses ring closures to convert the amide linkages into imide linkages.

Scheme 2 illustrates the expected structures and schematic synthetic route of colorless imide hybrid nanocomposite. The size and periodicity of the AONC and the diimide chain domains on the cross-link can be defined. The imide hybrid nanocomposites with a three-dimensional network are isotropic, and the bulky side group in the alicyclic dianhydrides reduces the chain packing between the organics. These structural features can reduce the optical anisotropy which is disadvantageous in optical applications. The optical and thermal properties of imide hybrid nanocomposites can be advanced by the simultaneous use of AONC and alicyclic dianhydrides. The chemical structure, thermal properties and optical characteristics are reported in this study.

Experimental

Materials

3-Aminopropyltrimethoxysilane (APTS, 97%, Aldrich), diphenylsilanediol (DPSD, 98%, TCI) 1,2,3,4-cyclobutanetetracarboxylic dianhydride (CBDA, 99%, Aldrich) and barium hydroxide monohydrate (Aldrich) were used without further purification. 5-(2,5-Dioxotetrahydrofuryl)-3-methylcyclohexene-1,2-dicarboxylic anhydride (DODCA, 95%, TCI) was purified by recrystallization from acetic anhydride and dried at 150 °C before use. 1-Methyl-2-pyrrolidinone (NMP, 99%, Aldrich) was purified by the usual manner and stored under nitrogen atmosphere. Other reagents and solvents were used as received.

Synthesis of AONC

The AONC 50 was prepared from APTS and DPSD. First, we mixed 7.17 g (4 mmol) of APTS with 0.02 g (0.01 mmol) of barium hydroxide monohydrate at 80 °C in a 250 mL two-necked flask. We then gradually added 8.65 g (4 mmol) of DPSD to the mixture over two hours to prevent self-condensation of DPSD. The solution was kept at 80 °C for a further two hours to progress the reaction. Next, we used vacuum heating to remove the methanol, which was a by-product of the condensation. The solution was then cooled to room temperature and filtered through a 0.45 μm Teflon filter to remove the barium hydroxide monohydrate. This process left a clear solution of viscous AONC 50. Depending on the DPSD concentration, we then prepared AONC 33 (DPSD, 4.325 g, 2 mmol) and AONC 41 (DPSD, 7.1 g, 3.3 mmol) (see Table 1).

Table 1 Formulation of amine functionalized oligosiloxane nanobuilding clusters (AONC)

Samples	APTS	DPSD	$Ba(OH)_2 \cdot H_2O$	mol% of DPSD
AONC 33	7.17 g	4.325 g	0.02 g	33.3
AONC 41	7.17 g	7.1 g	0.02 g	41.7
AONC 50	7.17 g	8.65 g	0.02 g	50

Fabrication of imide hybrid nanocomposite

The AONC–DODCA imide hybrid nanocomposites were prepared from AONC 50 and DODCA. First, we kept the mole ratio of the amine : anhydride groups at 1 : 1. We then separately dissolved 13.26 g (4 mmol of NH_2) of AONC 50 and 8.89 g (2 mmol) of DODCA in 1-methyl-2-pyrrolidinone. The solid content in the solution was 10 wt%. After vigorously stirring the mixture for 12 hours at 0 °C, the final solution was spin-coated on a silicon substrate or cast on a glass slide. The prepared films were dried at 60 °C for 3 hours and at 120 °C for another 3 hours in air. After curing the films at 300 °C for 2 hours in an N_2 atmosphere, we then obtained the final samples.

To fabricate the AONC–CBDA imide hybrid nanocomposites, we used the same procedure. We separately dissolved 13.26 g (4 mmol of NH_2) of AONC 50 and 3.93 g (2 mmol) of CBDA in 1-methyl-2-pyrrolidinone. The solid content in the solution was 10 wt%. We then followed the same curing steps.

Characterization

The ^{29}Si nuclear magnetic resonance (NMR) spectra were recorded using a Bruker FT 500 MHz instrument from a sample consisting of 30 vol% of the resin in chloroform-d. Chromium(III) acetylacetonate as a relaxation agent of silicon was added at a concentration of 30 mg l^{-1}. Pulse delays were 30 s, the sample temperature was 300 K, and TMS was used as a reference. Raman spectra were measured with a 488 nm Ar–Kr ion laser (Coherent Innova 70 series, Laser Innovations, Moorpark, CA) and double-grating monochromater (U-1000, Jovin Yvon, Inc., Edison, NJ). Fourier transform infrared (FT-IR) spectra of the synthesized materials were obtained by a JASCO FT-IR 460plus with a resolution of 4 cm^{-1}. All measurements were performed at 4000–400 cm^{-1}. The spectra of matrix assisted laser desorption and ionization–time of flight mass spectroscopy (MALDI-TOF MS) were obtained with a Voyager-DE STR 4700 proteomics analyzer (PerSeptive Biosystems, Framingham, MA) equipped with a nitrogen laser using a wavelength of 337 nm and a pulse width of 3 ns. The sample preparations for MALDI-TOF MS were as follows. The 2,5-dihydroxybenzoic acid (DHB, Aldrich) matrix solution was prepared by dissolving 20 mg in 1 mL of acetone. Matrix and AONC solutions were mixed in a 4 : 1 ratio. Solution droplet of the matrix–sample mixture were deposited on the sample plate target and allowed to dry at room temperature. Small angle neutron scattering (SANS) experiments were performed in the SANS instrument in the HANARO Reactor at the Korea Atomic Energy Research Institute (KAERI). The experimental set-up included a wavelength of 5.08 Å with a wavelength spread (FWHM) of 12%, and a detector–sample distance of 3 m. The scattering vector ranged between 0.04 $Å^{-1}$ and 0.25 $Å^{-1}$. The scattered neutrons were counted with a 2-D detector. After correction for detector efficiency and conversion to an absolute scale using the direct beam intensity, the 2-D intensity was circularly averaged.

Thermogravimetric analysis (TGA) and differential scanning calorimetry (DSC) measurements were performed under nitrogen atmosphere at a heating rate of 5 °C min^{-1} using a

Dupont 9900 analyzer. The transmission and near infrared absorption spectra of solutions and films were obtained using an ultraviolet–visible–near infrared (UV/VIS/NIR) spectrophotometer (Shimadzu, UV3101PC). The refractive index of solution and film was obtained by using an Abbe refractometer (Bellinghams Stanle Ltd. 60/ED) at 589.6 nm wavelength and a prism coupler (Pennington, Metricon 2010) at 632.8 nm wavelength. The birefringence (Δn), which is defined as the difference between the in-the-plane and out-of-plane refractive indices (the difference between n_{TE} and n_{TM}), was also calculated.

Results and discussion

Synthesis and structural analysis of AONC

AONC can be easily prepared in a single step by using the barium hydroxide monohydrate-catalyzed condensation reactions between APTS and DPSD. To avoid positively or negatively charged amines, we used both chloride-free condensation catalysts and organosilanediols, such as DPSD. Because the DPSD was already hydrolyzed and contained no chloride, the siloxane frames were formed mainly as a result of the condensation reaction between APTS and DPSD without hydrolysis. Barium hydroxide monohydrate is an effective catalyst that can activate a condensation reaction between APTS and DPSD, and it restricts self-condensation of the DPSD. The evidence for restricted self-condensation of DPSD is the very low water content, released from DPSD self-condensation, in the final solution. The main role of this catalyst is to stabilize the penta-coordinated state of APTS, an intermediate state between the two reactants and the condensate, and accelerate condensation between two different silanes.[17]

APTS was mixed with barium hydroxide monohydrate at 80 °C and the DPSD was very slowly added under reduced pressure. The final AONC was obtained after simple filtration with a 0.45 μm syringe filter. The MeOH, which is produced by condensation, could be easily removed by heating at 80–100 °C and under reduced pressure. A solventless, viscous and clear AONC solution was obtained. This method excludes hydrolysis of alkoxysilane so that no water and solvent are allowed in the siloxane backbone construction. As barium hydroxide monohydrate is insoluble in water and any alcohols, they only participate in condensation reactions and can be easily removed by filtration. Thus, amine groups in AONC can be safely preserved during reactions and complicated neutralization treatment can be omitted. Various AONC were synthesized by DPSD content changes.

To investigate the various structures of AONC, we chose the following three compositions for the molar ratios of APTS/(APTS + DPSD): 0.33 (AONC 33), 0.41 (AONC 41) and 0.5 (AONC 50). All the AONC comprised tetramers, pentamers, and hexamers; moreover, AONC 50 had the highest concentration of hexamers. To eliminate all the lower molecular-weight species except for hexamers, we used size exclusion chromatography after diluting AONC 50 in proper solvents. Thus, we obtained relatively homogeneous and uniform AONC and we are currently investigating how to produce better results.

FT-IR results of AONC show a strong and broad vibrational band (1000–1200 cm^{-1}) related to the siloxane backbone and small vibration bands of NH_2 ($\sim$3350 cm^{-1}: N–H stretch, and 1617 cm^{-1}: N–H bending). No vibrational bands related to NH_3^+ (3300–2600, 1975, 1606, 1505 cm^{-1}) and silanols were observed in any of the spectra. These results demonstrated that the siloxane framework was successfully formed and amino groups were unchanged in AONC.

The ^{29}Si NMR data shown in Fig. 1 also support the FT-IR results. D^n and T^n represent Si from DPSD and APTS, respectively, and the superscript n denotes the number of siloxane bonds of Si. The ratios of the D and T species in each composition are well matched to the starting batch. No peaks related to unreacted silanes (DPSD: −34 ppm, T^0: −42 ppm) were found in any of the spectra. The siloxane backbones in AONC were well established, by simply modified condensation reactions, in which hydrolysis and mineral acids such as HCl, H_2SO_4 and HNO_3 were not utilized. This result demonstrated the amine functionalized siloxane-based nanobuilding clusters were successfully prepared.

The size of AONC as determined by SANS is below 2 nm. The Guinier plots of the SANS data exhibit a single slope in the Guinier region, thereby revealing that AONC have structures. The gyration radii (R_g) of AONC were calculated using Guinier plots (scattered intensity ($I(q)$ *versus* q^2 (q = scattering vector)) in the Guinier region ($0.1 < R_g q < 1$). The AONC was diluted to 10 wt% concentration in acetone-d_6 to obtain a good contrast between AONC and the solvent. Fig. 2 shows the Guinier plots of scattered intensities from AONC. The gradients of the Guinier plots are negative and slightly increase with the DPSD content, indicating that the size of AONC increases slightly.

The sizes of AONC depending on their shapes were estimated from R_g. The diameters of spherical shaped AONC were about 2 nm. The SANS data for AONC were adequately fitted using a simple noninteracting hard sphere model with a diameter of about 2 nm. Thus, the sizes of AONC were below 2 nm. Moreover, the negligible variation in each gradient of the Guinier plot implies that the size of

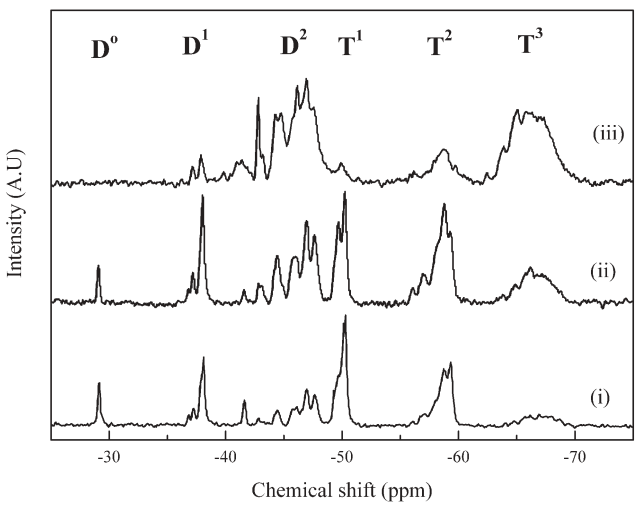

Fig. 1 The ^{29}Si NMR spectra of AONC 33 (i), AONC 41 (ii) and AONC 50 (iii).

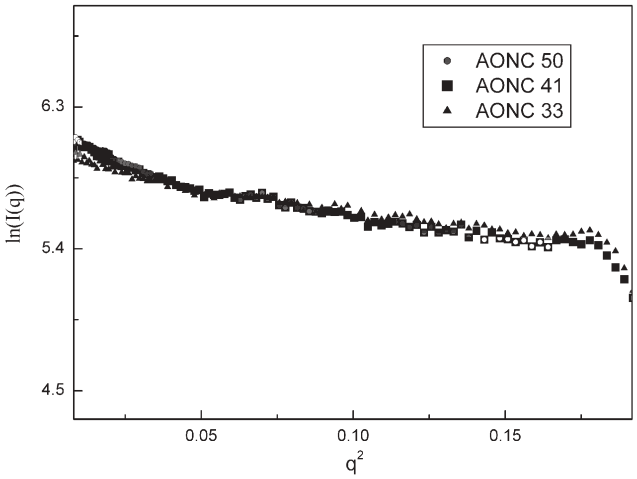

Fig. 2 Guinier plots ($I(q)$ *vs.* q^2) of the SANS data from AONC.

the AONC varied only slightly. This result suggests that the nanoclusters were well established.

The MALDI-TOF mass spectroscopy and Raman data support the SANS results. The Raman spectra (Fig. 3) of the AONC show that the AONC have linear siloxane backbones. There are no bands in any of the spectra that indicate the formation of cyclic siloxane rings or cage structures. On the basis of the Raman results, we considered only the linear species in the MALDI-TOF analysis for estimating the nanostructures of the AONC. Thus, it is found that the mainly formed AONC are linear or slightly branched tetramer, pentamer and hexamer structures from a combination of MALDI-TOF and Raman data.

MALDI-TOF data of AONC are shown in Fig. 4. As the DPSD content increases in AONC, the nanoclusters evolve from a tetramer to a hexamer structure. We found that AONC 33 has mainly tetramers and that AONC 50 has mainly hexamers. If we assume that most AONC have a linear siloxane backbone, the values of the *m*/*z* in the spectra exactly match the mass of tetramers, pentamers and hexamers. In the spectrum of AONC 33, as shown in Fig. 4b, the linear tetramer

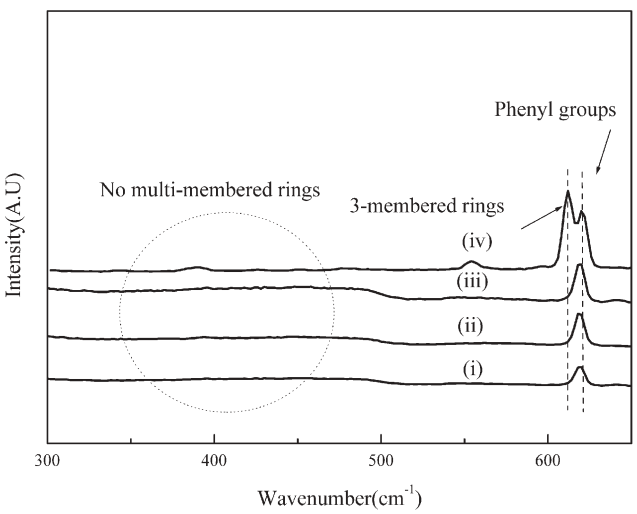

Fig. 3 Raman spectra of AONC 33 (i), AONC 41 (ii), AONC 50 (iii) and hexaphenylcyclotrisiloxane (HPCS) (iv). HPCS (3-membered ring) was used as a reference substance for cyclic ring structured oligosiloxanes.

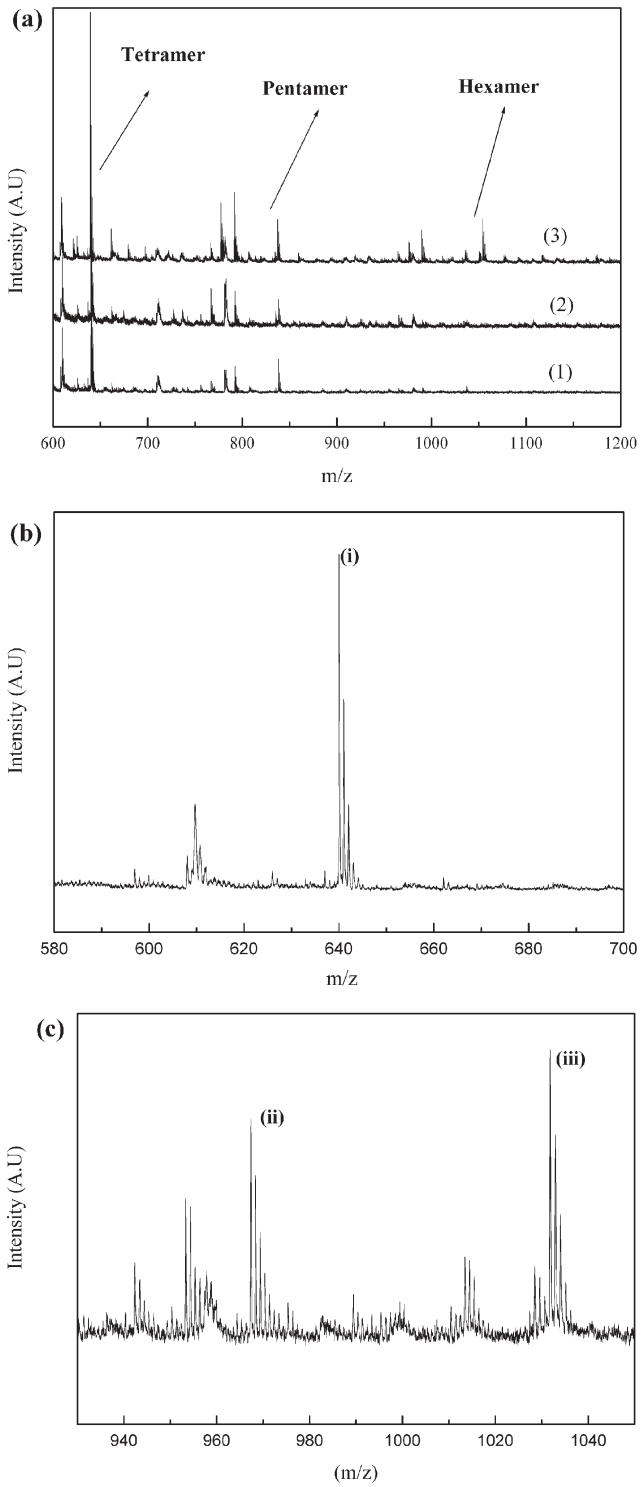

Fig. 4 (a) MALDI-TOF mass spectra of AONC 33 (1), AONC 41 (2) and AONC 50 (3). Peaks corresponding to tetramer, pentamer and hexamer are represented. Detailed spectra of various AONC: (b) linear tetramer (m/z = 644 ((i), three APTS and one DPSD)), (c) two linear hexamers (m/z = 1040.6 ((ii), three APTS and three DPSD), 975.2 ((iii), four APTS and two DPSD)).

(m/z = 644) has three APTS and one DPSD, and the small amount of pentamers (m/z = 777.3, 842) has three APTS and two DPSD. In the spectrum of AONC 50, as shown in Fig. 4c, there are two different hexamers (m/z = 975.2, 1040.6). These results show that we can successfully obtain AONC, and that there are two or three amine groups in the AONC that can act as nanoconstruction sites.

Fabrication of imide hybrid nanocomposites

AONC–DODCA imide hybrid nanocomposites. To fabricate imide hybrid nanocomposites, we used a general method of organic polyimide synthesis. The AONCs reacted with the DODCA to form an AONC amic acid solution as an intermediate state before forming the imide hybrid nanocomposite. In this step, each AONC was connected to short amide chains. The amic acid groups were then changed into imide groups after thermal imidization. Finally, we fabricated the imide hybrid nanocomposites in which each AONC was cross-linked with short diimide chains.

AONC–CBDA imide hybrid nanocomposites. The AONC–CBDA imide hybrid nanocomposites were prepared in the method described above. The amic acid groups were well formed after the condensation reaction, and they were easily changed into imide groups by thermal imidization. These nanocomposites had shorter diimide chains than the AONC–DODCA imide hybrid nanocomposites.

FT-IR characterization

Fig. 5 shows FT-IR spectra of the imide hybrid nanocomposites that we prepared from AONC 50 and DODCA. The characteristic absorption band of the siloxane bonds in the AONCs was clearly observed around 1000 cm^{-1} to 1200 cm^{-1}. Fig. 5a shows an FT-IR spectrum of the nanocomposites that we prepared by mixing AONC 50 and DODCA at 0 °C for 12 hours. At this step, we found characteristic amic acid absorptions at 1650 cm^{-1} and 1720 cm^{-1} (both C=O in amide), and the formation of the amide linkage between AONC and DODCA was revealed. In contrast, the samples cured at either 120 °C or 300 °C show characteristic imide absorptions at 1370 cm^{-1} (C–N in imide) and 1780 cm^{-1} (C=O in imide). Because the imidization process involved water from cyclization, we observed imide bonds in the sample cured at 120 °C (Fig. 5b). The completely imidized sample was obtained after curing at 300 °C in an N_2 atmosphere (Fig. 5c). In the case of the AONC–CBDA imide hybrid nanocomposites, we observed the same imide and siloxane characteristic absorptions. These FT-IR results demonstrate that the imide hybrid nanocomposites were well fabricated.

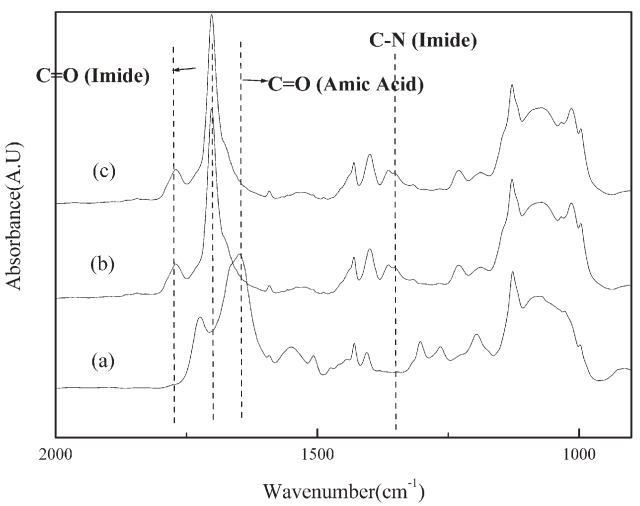

Fig. 5 FT-IR spectra of imide nanocomposite prepared from AONC 50 and DODCA: (a) mixed at 0 °C for 12 hours, (b) cured at 120 °C for another 2 hours and (c) cured at 300 °C for another 2 hours (in N_2) The imidization started at 120 °C and was completed at 300 °C. The existence of a C–N bond in the imide nanocomposite reveals that amine groups in AONC are maintained after condensation.

Thermal properties of imide hybrid nanocomposites

The thermal properties of imide hybrid nanocomposites were characterized by TGA. Fig. 6 showed TGA curves of AONC–DODCA imide hybrid nanocomposites and AONC 50. As expected, after the imide linkages were formed in the nanocomposites, the thermal stabilities were enhanced. Their 5% weight loss temperatures under N_2 were approximately 430 °C. A rapid weight loss for AONC 50 was observed above 390 °C due to decomposition of the remaining alkoxy groups.

The AONC–CBDA imide hybrid nanocomposites behaved similarly, except for the increase in temperature for the 5% weight loss. The temperature was around the value generally expected for alicyclic polyimides.[21,22]

Table 2 lists the thermal properties of the imide hybrid nanocomposites, as evaluated by TGA. Unfortunately, the extensive difference in structures, synthetic methods, variables and chemical components does not allow a simple comparison between imide hybrid nanocomposites and other alicyclic polyimides. However, the decomposition temperatures (T_d) of the nanocomposites, at which a 10% weight loss was observed, are higher than those of the polyimides prepared from alicyclic dianhydride. The incorporation of AONC can retard the decomposition at lower temperatures due to the low molecular

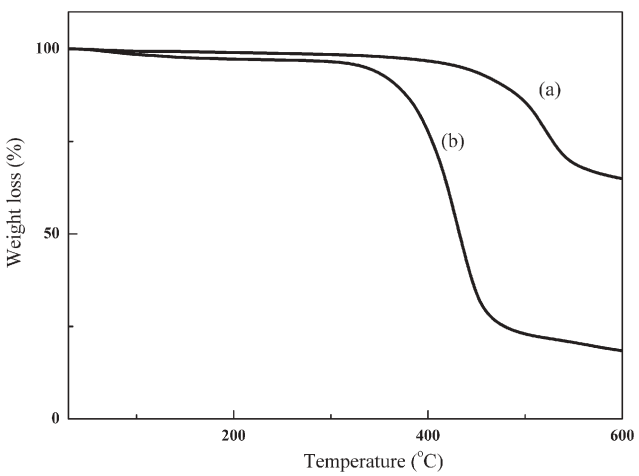

Fig. 6 TGA curves of (a) an AONC 50–DODCA imide hybrid nanocomposite and (b) AONC 50.

Table 2 Thermal stabilities of AONC and imide hybrid nanocomposites

Sample	T_d(5%)/°C[a]	T_d(10%)/°C[b]
AONC 33	360	380
AONC 41	360	385
AONC 50	368	405
AONC 50/DODCA	430	475
AONC 50/CBDA	450	480

[a] Temperature at 5% weight loss; [b] temperature at 10% weight loss determined by TGA at a heating rate of 10 °C min^{-1} under N_2.

weight of the short imide segments in the nanocomposites. The TGA results show that the thermal stability is excellent and stable up to about 450 °C, and sufficient for microelectronic and optoelectronic applications.

Optical properties of imide hybrid nanocomposites

The optical transmission spectra of imide hybrid nanocomposite films are shown in Fig. 7. The samples were prepared by spin coating on a quartz substrate. The thickness of the prepared films ranged from 2.31 μm to 3.23 μm. Both types of nanocomposite had excellent transmittance over 90% in the visible range and were colorless. The imide hybrid nanocomposites films prepared from DODCA and CBDA have cutoffs at 330 nm and 310 nm, respectively. These values are reasonable compared to other values in the literature.[12,18] We defined the cutoff wavelength as the point where the transmittance drops below 1% in the spectrum.

The refractive indices of imide hybrid nanocomposites were also studied. In-plane and out-of-plane refractive indices (n_{TE} and n_{TM}) measured at 632.8 nm wavelength are summarized in Table 3. In addition, the refractive indices of AONC were measured at 589.6 nm by using an Abbe refractometer. Samples were prepared by spin coating on p-type Si (100) wafers. The refractive indices of the nanocomposites films and AONC are linearly proportional to the DPSD contents in AONC. As the DPSD increased, there was an increase in the electronic polarizability, which was due to

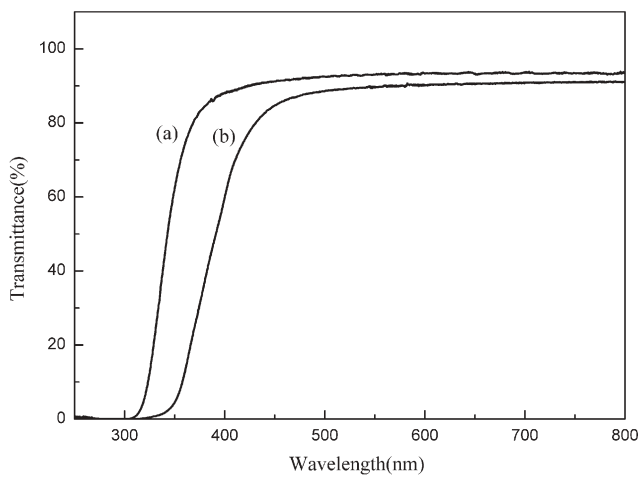

Fig. 7 UV-Vis spectra of (a) an AONC 50–CBDA imide hybrid nanocomposite and (b) an AONC 50–DODCA imide hybrid nanocomposite.

Table 3 The refractive indices and birefringence of AONC and imide hybrid nanocomposite films

Sample	Thickness/μm	n_{TE}[a]	n_{TM}[b]	n_{AV}[c]	Δn[d]	ε[e]
AONC 33	—[f]	—	—	1.5174[g]	—	—
AONC 41	—[f]	—	—	1.5387[g]	—	—
AONC 50	—[f]	—	—	1.5576[g]	—	—
AONC 50/DODCA	2.31	1.5703	1.5682	1.5696	0.002	2.71
AONC 50/CBDA	3.23	1.5528	1.5498	1.5518	0.003	2.65

[a] The in-plane refractive indices. [b] The out-of-plane refractive indices. [c] Average refractive index: $n_{AV} = (2n_{TE} + n_{TM})/3$. [d] Birefringence: $\Delta n = n_{TE} - n_{TM}$. [e] Optically estimated dielectric constant: $\varepsilon = 1.10 n_{AV}^2$. [f] Solutions. [g] Measured using an Abbe refractometer.

the larger phenyl content, as well as in the density, which was due to the higher condensation degree. Therefore, the nanocomposites with AONC 50 show the highest value of the refractive index. Because the refractive indices of the AONC can vary widely from 1.5174 to1.5576 at a wavelength of 589.6 nm, those of the imide hybrid nanocomposites with AONC can be widely and easily controlled in the range of 1.5322 to 1.5703 (AONC–DODCA) at a wavelength of 632.8 nm. This result is promising for optical waveguide applications.

For all nanocomposites, the value of n_{TE} was slightly larger than the value of n_{TM}. This phenomenon is a characteristic property of polyimides prepared by means of on-substrate imidization. We estimated the birefringences (Δn) of the imide hybrid nanocomposite films to be 0.002 and 0.003 which are smaller than the birefringences of pure polyimides and polyimide–silica hybrid materials. These small birefringences indicate that imide hybrid nanocomposites have low polarizability, anisotropy and three dimensional network structures.

From structural analysis, we know that AONC have more than three amine groups. As a result, the AONCs generate three-dimensional random networks. The unsymmetrical structure and the large bulky alicyclic side groups reduce the anisotropy.

The dielectric constant (ε) of materials at optical frequencies can be estimated from the refractive index n according to Maxwell's equation, $\varepsilon \approx n^2$. The value of ε around 1 MHz has been evaluated as $\varepsilon \approx 1.10\ n_{AV}^2$, including an additional contribution of approximately 10% from the infrared absorption.[23] In the case of the AONC 50–DODCA and the AONC 50–CBDA imide hybrid nanocomposites, n_{AV} values of 1.5696 and 1.5518 can be translated into dielectric constants of 2.71 and 2.65, respectively. These values are lower than the optically estimated values of conventional semiaromatic polyimides (2.83).[12] Moreover, these results indicate that imide hybrid nanocomposites are good candidates for low dielectric interlayer materials.

Conclusions

This research demonstrates the simple synthesis of AONC and imide hybrid nanocomposites prepared from AONC and alicyclic dianhydrides. Using a modified sol–gel process that requires no water or solvent, we successfully synthesized new AONC in a single-step condensation reaction. In addition, the

AONC prepared with this method are siloxane-based nanoclusters below 2 nm diameter. and they require no neutralization treatments with NH_3^+ to maintain their amino functionality. The imide hybrid nanocomposites prepared from AONC and alicyclic dianhydrides (DODCA and CBDA) have good thermal stability with a 5% weight loss at a temperature of around 430 °C. They also have excellent optical properties; for instance, high water transparency (above 90% in the visible region and a UV cutoff at around 310 nm), a widely tunable refractive index and a low birefringence (about 0.002). The optically estimated dielectric constant is as low as 2.65. Colorless imide hybrid nanocomposites prepared from AONC and alicyclic dianhydrides can be used for promising transparent substrates.

Acknowledgements

This work was supported by the Sol–Gel Innovation Project (SOLIP) of the Ministry of Commerce, Industry and Energy of Korea. The authors are grateful to Baek-Seok Seong of the Korea Atomic Energy Research Institute (KAERI) for useful discussion and help with operating the SANS instruments in HANARO.

References

1 R. Tamaki, Y. Tanaka, M. Z. Asuncison, J. Choi and R. M. Laine, *J. Am. Chem. Soc.*, 2001, **123**, 12416–12417.
2 Y. Lu, Y. Yang, A. Sellinger, M. Lu, J. Huang, H. Fan, R. Haddad, G. Lopez, A. R. Burns, D. Y. Sasaki, J. Shelnutt and C. J. Brinker, *Nature*, 2001, **410**, 913–917.
3 Q. Xu, L. Li, X. Liu and R. Xu, *Chem. Mater.*, 2002, **14**, 9, 549–555.
4 S. Kalluri, Y. Shi, W. H. Steier, Z. Yang, C. Xu, B. Wu and L. R. Dalton, *Appl. Phys. Lett.*, 1994, **65**, 2651–2653.
5 N. Steunou, S. Forster, P. Florian, C. Sanchez and M. Antonietti, *J. Mater. Chem.*, 2002, **12**, 3426–3430.
6 C. Sanchez, B. Julian, P. Belleville and M. Popall, *J. Mater. Chem.*, 2005, **15**, 3559–3592.
7 S. Bocchini, G. Fornasieri, L. Rozes, S. Trabelsi, J. Galy, N. E. Zafeiropoulos, M. Stamm, J.-F. Gerard and C. Sanchez, *Chem. Commun.*, 2005, 20, 2600–2602.
8 F. J. Feher and K. D. Wyndham, *Chem. Commun.*, 1998, 3, 323–324.
9 A. Hartl, E. Schmich, J. A. Garrido, J. Hernando, S. C. R Catharino, S. Water, P. Feulner, A. Kromka, D. Steinmuller and M. Stutzmann, *Nat. Mater.*, 2004, **3**, 736–742.
10 J. S. Park, Y.-J. Lee and K. B. Yoon, *J. Am. Chem. Soc.*, 2004, **126**, 1934–1935.
11 R. Ohta, N. Saito, Y. Inoue, H. Sugimura and O. Takai, *J. Vac. Sci. Technol., A*, 2004, **22**, 2005–2009.
12 J. Naciri, J. Y. Fang, M. Moore, D. Shenoy, C. S. Dulcey and R. Shashidhar, *Chem. Mater.*, 2000, **12**, 3288–3295.
13 N. Liu, R. A. Assink, B. Smarsly and C. J. Brinker, *Chem. Commun.*, 2003, 1146–1147.
14 C. Feger and H. Franke, in *Polyimides Fundamentals and Applications*, ed. M. K. Ghosh, and K. L. Mittal, Marcel Dekker, New York, 1996, p. 7.
15 C. C. Chang and W. C. Chen, *Chem. Mater.*, 2002, **14**, 4242–4248.
16 W. Chen, W. C. Wang, W. H. Yu, E. T. Kang, K. G. Neoh, R. H. Vora, C. K. Ong and L. F. Chen, *J. Mater. Chem.*, 2004, **14**, 9, 1406–1412.
17 M. Nandi, J. A. Conklin, L. Salvati and A. Sen, *Chem. Mater.*, 1991, **3**, 201–206.
18 Y. Watanabe, Y. Shibasak, S. Ando and M. Ueda, *J. Polym. Sci., Part A: Polym. Chem.*, 2004, **42**, 144–150.
19 Y.-T. Chern and H.-C. Shiue, *Macromolecules*, 1997, **30**, 4646–4651.
20 C.-M. Leu, G. M. Reddy, K.-H. Wei and C.-F. Shu, *Chem. Mater.*, 2003, **15**, 2261–2265.
21 Y. Watanabe, Y. Sakai, Y. Shibasak, S. Ando and M. Ueda, *Macromolecules*, 2002, **35**, 2277–2281.
22 J. Li, K. Kudo and S. Shiraish, *Macromol. Rapid Commun.*, 2000, **21**, 1166–1170.
23 D. Boese, H. Lee, D. Y. Yoon, J. D. Swallen and J. F. Rabolt, *J. Polym. Sci., Part B: Polym. Phys.*, 1992, **30**, 1321–1327.

